LBL-31208
UC-110

# Lawrence Berkeley Laboratory

UNIVERSITY OF CALIFORNIA

## Materials & Chemical Sciences Division

**Activity Report: A Report of Research Activity in Fiscal Years 1986 and 1987**

P.N. Ross, B. Beard, and M Sattler

January 1988

**Prepared for the U.S. Department of Energy under Contract Number DE-AC03-76SF00098**

## DISCLAIMER

LBL--31208

DE92 009486

# Activity Report

A Report of Research Activity
in Fiscal Years 1986 and 1987

Prepared for the Morgantown Energy Technology Center
Morgantown, W. VA

by

Philip N. Ross
Principal Investigator

and

Bruce Beard and Margaret Sattler
Postdoctoral Research Associates

Materials Sciences Division
Lawrence Berkeley Laboratory
Berkeley, CA 94720

January 1988

This work was supported by the Assistant Secretary of Fossil Energy, Office of Fuel Cells, Advanced Concepts Division of the U.S. Department of Energy under contract DE-AC03-76SF00098.

This report summarizes the last elements of work conducted in this program prior to its termination at the end of FY '87. The work was primarily an analysis of a fuel cell electrocatalyst using electron microscopy. The catalyst was a three component system containing Pt-Co-Ni (3:2:2 atomic ratios) dispersed on an amorphous carbon support in unknown phases, supplied to us by Giner Inc. (designated as their sample no. G82-5-19). The preparation of this catalyst is proprietary, (patent pending). Our objective was to analyze the catalyst by a variety of techniques to determine, to the greatest extent possible, the distribution of the three elements on the carbon support along with identification of their chemical states and phases.

The methods of analysis used were extended x-ray absorption fine structure spectroscopy (EXAFS), performed by us at the Stanford Synchrotron R diation Laboratory (SSRL), high resolution transmission electron microscopy (HRTEM) and high resolution x-ray mapping (EDAX), performed by us on microscopes at the LBL National Center for Electron Microscopy (NCEM).

## 2. Technical Progress Summary

### 2.1 EXAFS

The experimental procedures and methods of data reduction are described in LBL-28663 [1]. EXAFS spectra were obtained on four catalysts received by us, and unreduced catalyst and three reduced at 500, 700 and 900°C. The purpose of examining different reduction temperatures was to determine what reduction conditions are needed to form Pt-alloy particles. The Co-edge and Ni-edge EXAFS spectra are shown in Figs. 1 and 2, respectively. The Co-edge spectra, and the progressive change with heat-treatment, are very similar to the spectra we obtained with a LBL prepared Pt-Co binary catalyst, reported in LBL-28663. These

spectra indicate Co is present in the unreduced catalyst primarily as an amorphous oxide, and is reduced to a Pt-Co alloy phase only at 900°C and above. However, the relative fraction of Co present reduced to a Pt-Co phase is lesser in the Giner catalyst than in the LBL catalyst, which is not surprising due to the higher Co/Pt ratio in the Giner catalyst (factor of two). On the other hand, the Ni-edge spectra do not change with increasing heat-treatment, nor do they show the appearance of the peak at ca. 2.5 Å characteristic of a Pt-Ni coordination. The radial distribution function for the Ni-edge does not match that for NiO or for metallic Ni, so the phase of the Ni is indeterminate.

**2.2 HRTEM**

As described above, the EXAFS data indicated that a Pt-Co alloy phase was formed after reduction at 900°C, but the Ni remained in an oxidized state in a separate phase. The EXAFS spectra did not, however, permit a clear identification of the stochiometry of the Pt-Co alloy. Further, because EXAFS is a volume integrative technique, we do not learn about the spatial distribution of the Pt-Co phases on the carbon surfaces, e.g. are they well dispersed or highly aggregated. An understanding of the spatial distribution of the Pt-Co phases, as well as the identification of the phase of single particles, was sought by the use of HRTEM. In this case, we heat treated the unreduced catalyst from Giner ourselves at 900 and 1200°C, the latter to produce larger crystallites of the Pt-Co phase.

An investigation by HRTEM of these samples was performed to define the microstructure of the small Pt-Co particles. In particular, atomic resolution at the surfaces was preferred and so the Atomic Resolution Microscope (ARM) operating at 1000kV accelerating voltage was utilized as well as the high resolution microscope JEOL 200CX at 200kV accelerating voltage. Preparation of samples consisted of crushing the catalyst material

and of dispersing the fine powder on specially prepared microscope holey carbon or holey silica/gold grids [2]. A typical micrograph of each of these annealed samples is given in Figures 3 and 4. For comparison, at least one of the Pt-Co particles in each figure is oriented toward <110> so that the {222} planes are visible. As we describe in detail below, the particles exhibit the face centered cubic (FCC) random alloy structure when reduced at 900°C and the $L1_2$ ordered alloy structure ($Pt_3Co$) when reduced at 1200°C.

Further shape features can be observed for the Pt-Co particles produced by reduction at 900°C. The particles in Figure 3, for example, show surface facets that are outlines by the {111} planes. However, the surface planes of these particles are not limited to (111) nor are they dominated by any specific plane and include such other low order planes as (100) and (110) even though these facets may be only a few atoms in breadth. Because the facets of these catalyst particles are abundant yet quite small, and in fact appear in two dimensions to be mere atomic steps, then the shape of these particles seems to be a pseudo-sphere rather than a theoretical equilibrium shape such as an icosahedron or a cubo-octahedron [3]. Dark field electron microscopy reveals a thickness change from the center of the particles to the edge, thus confirming the spherical shape over a flat shape. The average size of particles reduced at 900°C is $46\,\AA$.

Different surface features are recognizable on the $Pt_3Co$ particles that were formed by reduction at 1200°C. The particle in Figure 4 is oriented so that its zone axis is <110> which is the same orientation as the small Pt-Co particle in Figure 3 marked by the arrow. The basic symmetry difference between the two particles is best demonstrated through the Fourier transforms (diffraction patterns) taken of each particle and shown in the figures. The Fourier transform is obtained because of the regularity of the lattice, i.e., the lattice fringes visible in

the micrograph. For the 900°C reduction, Figure 3, the {111} planes and the {200} planes seen from the transform form the image of the particle. This pattern is typical for <110> oriented FCC solid. However, for the particle produced by reduction at 1200°C, Figure 4, the image and Fourier transform of the particle are somewhat different. Details of the diffraction pattern and the unit cell are shown in Figure 5 for clarity. Around the central beam of the diffraction pattern the {111} planes are visible and comparable to the diffraction pattern, shown in Figure 3. However, lattice spots are also visible from {100} and {110} planes. In an FCC pure metal, these reflections are forbidden. Their appearance is characteristic of the $L1_2$ ordered structure (usually referred to as the superlattice reflections). The unit cell for $L1_2$ structure of $Pt_3Co$ is shown in Figure 3c.

Further lattice information is available from Figure 4 when measurements of the lattice fringe spacings of the electron micrograph image are compared with those from the diffraction pattern. Note that the original diffraction pattern, Figure 3a, shows the amorphous rings of the carbon substrate which acts as an internal calibration in determining lattice fringe spacings. Fringes having $2.2\,\AA$ spacings were identified as (111) planes of the $Pt_3Co$ lattice. There were patches of fringes on the particle having a rectangular pattern measuring $3.6\,\AA$ by $2.8\,\AA$. These lattice fringes represent the (110) and (100) normally "forbidden" reflections for FCC metals. Additionally, upon closer inspection of the {111} lattice fringes at the edges of the particle, a noticeable widening of the lattice spacing is measured. These fringes are approximately $2.5\,\AA$ apart and only 3 or 4 can be observed at this spacing. This measurement is consistent with the d-spacing for {111} planes in CoO. Since these fringes appear parallel to the {111} planes of $Pt_3Co$, then it is conceivable that an atomically thin layer of CoO is epitaxially grown on this particle. We had studied the oxidation of $Pt_3Co$ bulk alloy at low

pressure ($< 10^{-6}$ torr) of oxygen [4] and found that thin films of CoO grow epitaxially on the surface. The most probable explanation of these CoO films on the $Pt_3Co$ particles is surface oxidation in the microscope caused by heating of the particles by the electron beam and reaction with residual oxygen in the relatively low vacuum in the sample stage ($10^{-8}$ torr).

Measured d-spacings from the diffraction pattern compare favorably to the values reported for reference materials:

| | | | |
|---|---|---|---|
| 1. | turbostratic C | 2.08 Å | (2.08 Å) |
| 2. | (111) $Pt_3Co$ | 2.23 | (2.22) |
| 3. | (110) superlattice | 2.74 | (2.72) |
| 4. | (100) superlattice | 3.86 | (3.85) |
| 5. | (111) CoO | 2.50 | (2.46) |

The numbers in parentheses are figures taken from the x-ray powder diffraction files. Additional microdiffraction data were obtained from other regions of the sample reduced at 1200°C to give a statistical average of all particle unit cell lattice spacings present in the material. All of the microdiffraction patterns in the appropriate orientation showed the forbidden spots associated with the $L1_2$ structure.

The surface features of the annealed (1200°C) $Pt_3Co$ particle are easily observed in Figure 4. Dominant (111) surface planes occur over four facets of the particle as well as two large (100) planes. However, the rounding at the edges between these planes indicates the presence of small (110) surface regions. Weak beam dark field microscopy [1] was also performed for morphology determination of these particles. This method is simpler than ARM imaging and many more particles can be analyzed. It is not as sensitive as ARM to detailed surface features, like small (110) facets formed at the intersection of (100) and (111) planes. It is, however, useful for qualitative shape determination, which can be important in

determining general trends in structural changes. A relatively large number (ca. 50) of particles were characterized by this method as predominantly truncated cubo-octahedrons, which is contrast to the pseudo-sphere shapes of particles in the catalyst reduced at 900°C.

**2.2 EDAX**

The elemental distribution of Pt, Co and Ni on the amorphous carbon support was observed using x-ray emission mapping in a JEOL 200 CX microscope with a Kevex Si (Li) solid state detector. For the samples that were reduced at temperatures below 900°C, there was little or no overlap between the Pt, Co and Ni maps, e.g. Co and Ni emission was highly dispersed over the carbon while Pt emission showed discrete particles. However, for the samples reduced at 900°C and 1200°C, the Co and Ni maps showed formation of distinct particles which mapped onto the Pt particles. Figure 6 shows the resulting x-ray maps for Pt, Co, and Ni as well as the secondary electron image of the same area in the sample reduced at 1200°C. The dark particles in the secondary electron image may be reasonably assumed to be metallic Pt-rich particles. Wherever these metallic particles are located in the carbon matrix, there is generally also x-ray emission intensity for all three elements, Pt, Co and Ni. The converse is also true, that there are little or no regions of Co and Ni x-ray emission where there is no Pt x-ray emission. The latter observation is particularly important because secondary excitation of the Co and Ni K-levels by high energy x-rays emitted from Pt occurs when the electron beam is on a Pt particle regardless of where the Co and Ni phases are located (in this scale of distance). K-shell emission from Co and/or Ni is not capable of exciting the L-shell emission from Pt that is used for the mapping.

Thus, the EDAX mapping is complementary to the EXAFS analysis, and shows that with a sufficiently high reduction temperature one can form metallic particles containing all three elements, i.e. a ternary Pt-Co-Ni alloy. However, the resulting particle size is quite large, typically 200 - 500 Å.

## 3.0 Conclusions and Recommendations

The combined analysis by EXAFS, HRTEM and EDAX indicates that a Pt-Co-Ni ternary alloy phase is formed only after reduction at the relatively high temperature of 1200°C. This high reduction temperature causes rather severe particle growth and produces Pt-Co-Ni particles of relatively large particle size, e.g. 200 - 500 Å. Reduction at lower temperature produces some Pt-Co binary alloy crystallites, which are predominantly of the composition $Pt_3Co$, but leaves a large quantity of Co and Ni in non-metallic form. The Ni-phase appears to be the more difficult to reduce. It is recommended that a different Ni salt be used in the catalyzation, one with ligands that are more easily reduced or lost.

## References


1) B. Beard and P. Ross, "The Structure and Activity of Pt-Co Alloys as Oxygen Reduction Catalysts", Lawrence Berkeley Laboratory Report LBL-28663, 1986.

2) M. Sattler and P. Ross, Ultramicros., 20, 21 (1986)

3) W. Romanowski, Surf. Sci. 18, 373 (1969).

4) U. Bardi, B. Beard and P. Ross, "Surface Oxidation of a Pt-20% Co Alloy: An X-Ray Photoelectron Spectroscopy and Low Energy Electron Diffraction Study on the [100] and [111] Oriented Single-Crystal Surfaces", Lawrence Berkeley Laboratory Report LBL-22205, 1987.

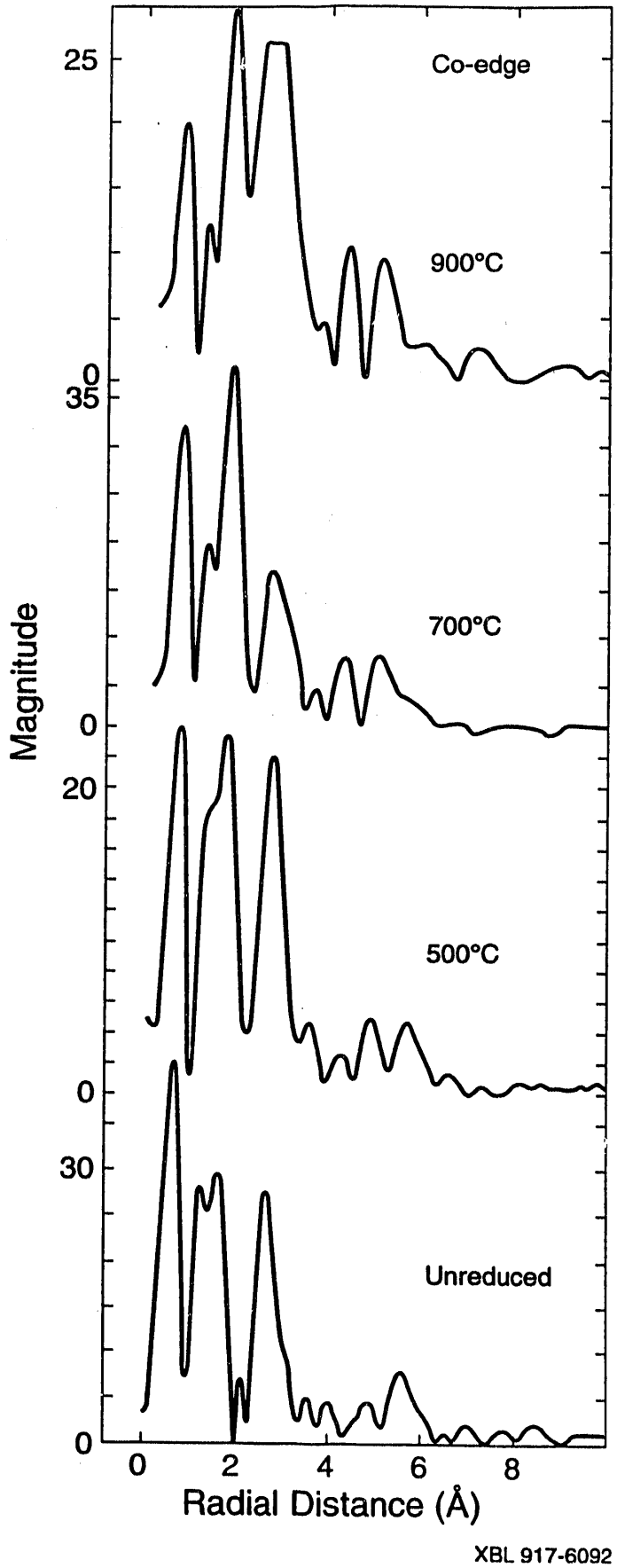


Figure 1. Radial distribution functions from the EXAFS spectra above the Co K-edge in Giner G82-5-19 Pt-Co-Ni catalyst following reduction at different temperatures.

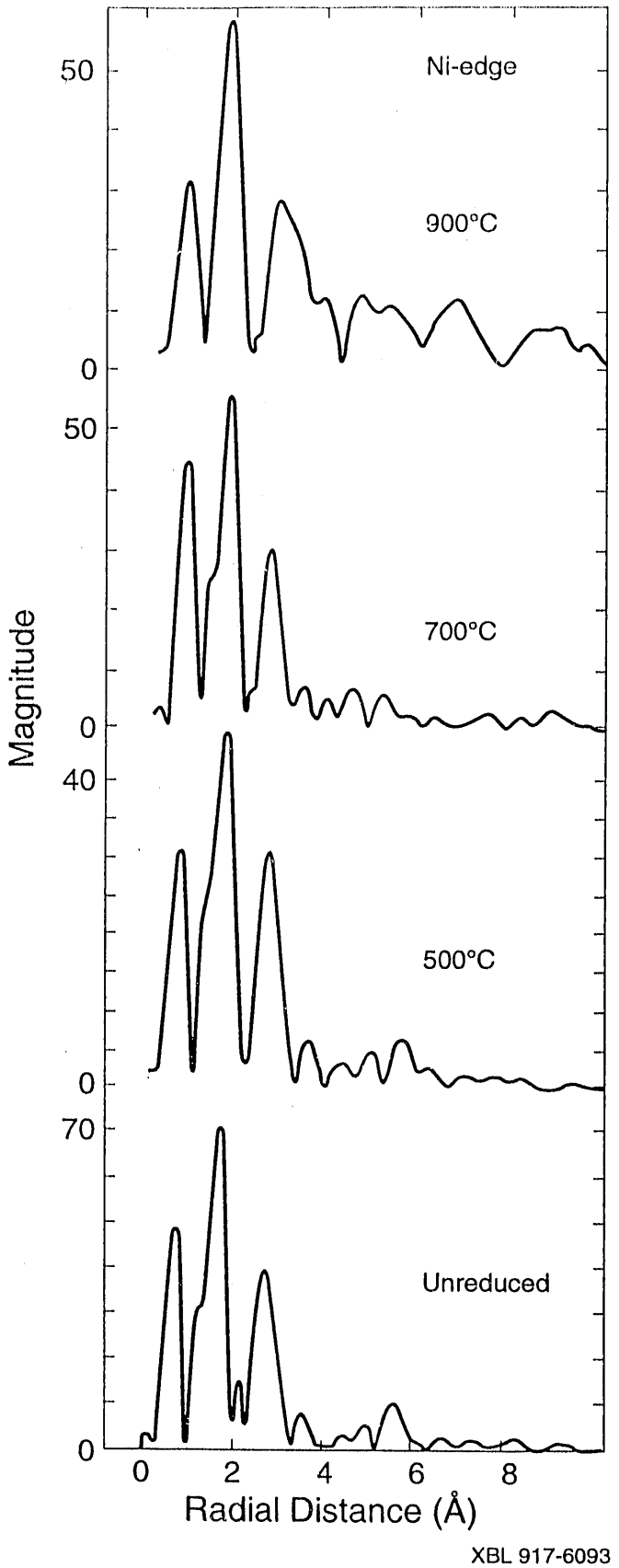


Figure 2. Radial distribution functions from the EXAFS spectra above the Ni K-edge in Giner G82-5-19 Pt-Co-Ni catalyst following reduction at different temperatures.

a

b

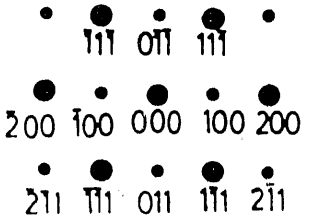


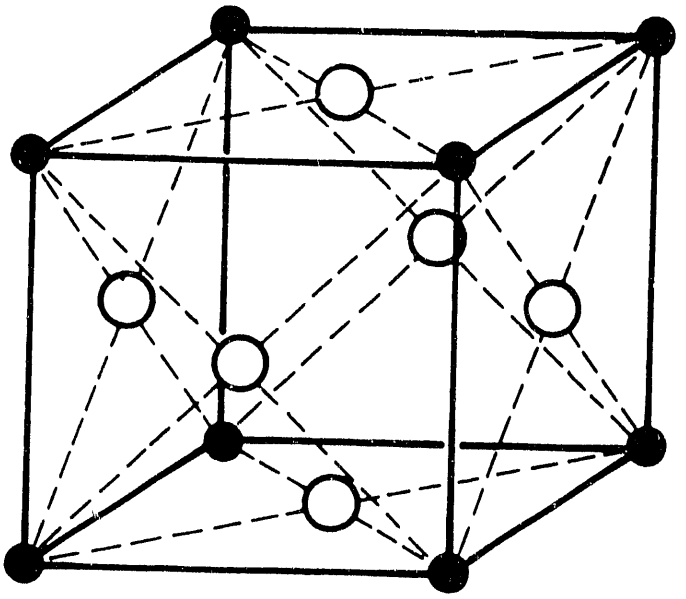

c

Figure 3: a) Diffraction pattern of $L1_2$ $Pt_3Co$ particle of Figure 2 in <110> orientation; b) Enlarged schematic of the diffraction pattern in a; c) Unit cell of $L1_2$ $Pt_3Co$ where Co atoms occupy the corners of the cell and Pt atoms the face centers.

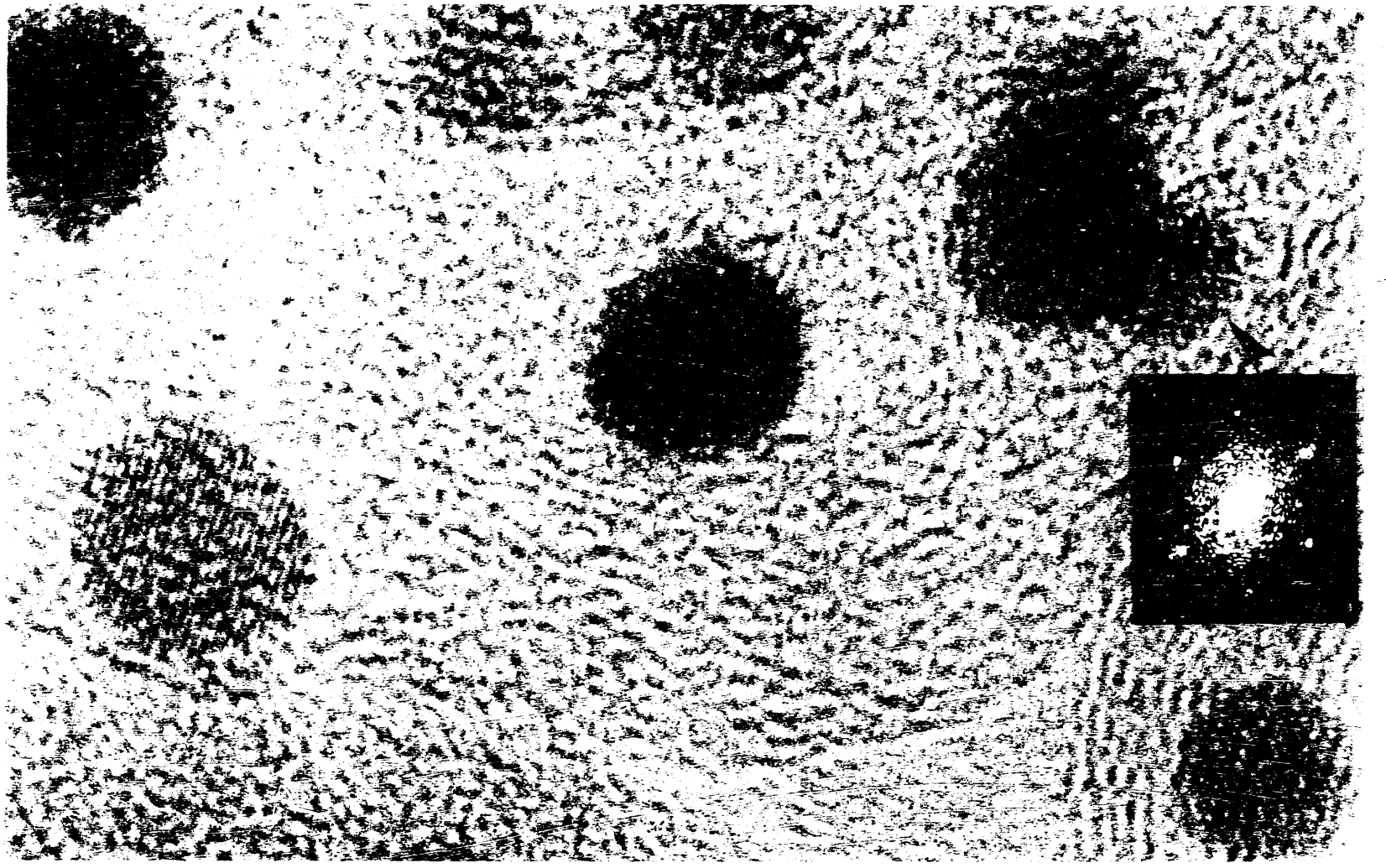

XBB 865-3995

Figure 4: $Pt_3Co$ on C catalyst sample annealed at 900°C. Particles contain lattice fringes from {111} planes. Fourier transform having <110> orientation is given for one of the particles.

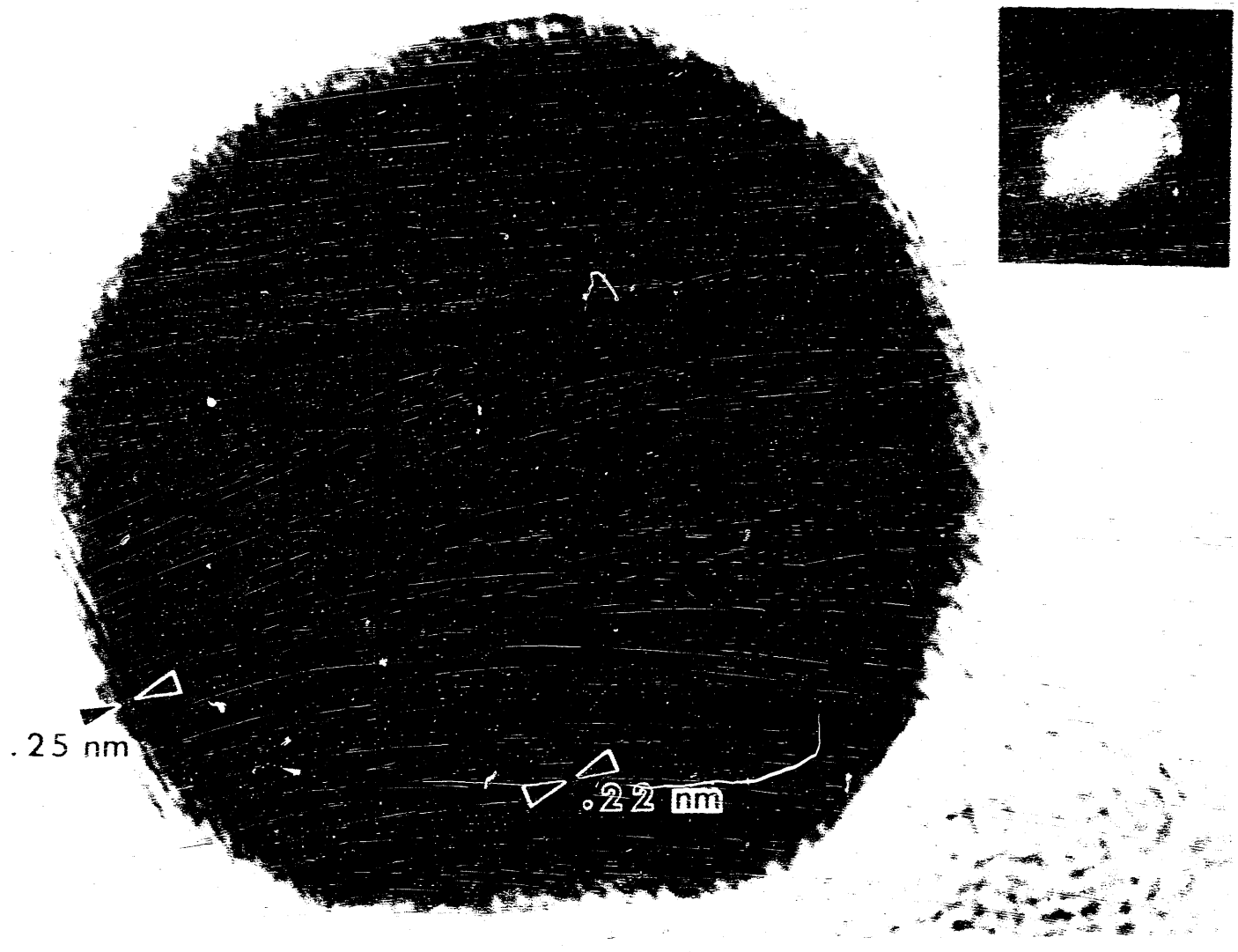


XBB 865-3996

Figure 5: Micrograph of catalyst sample annealed at 1200°C showing $Pt_3Co$ particle at edge of C substrate. Fourier transform shows lattice fringes arising from (111) planes as well as (100) and (110) forbidden planes. **10 nm**

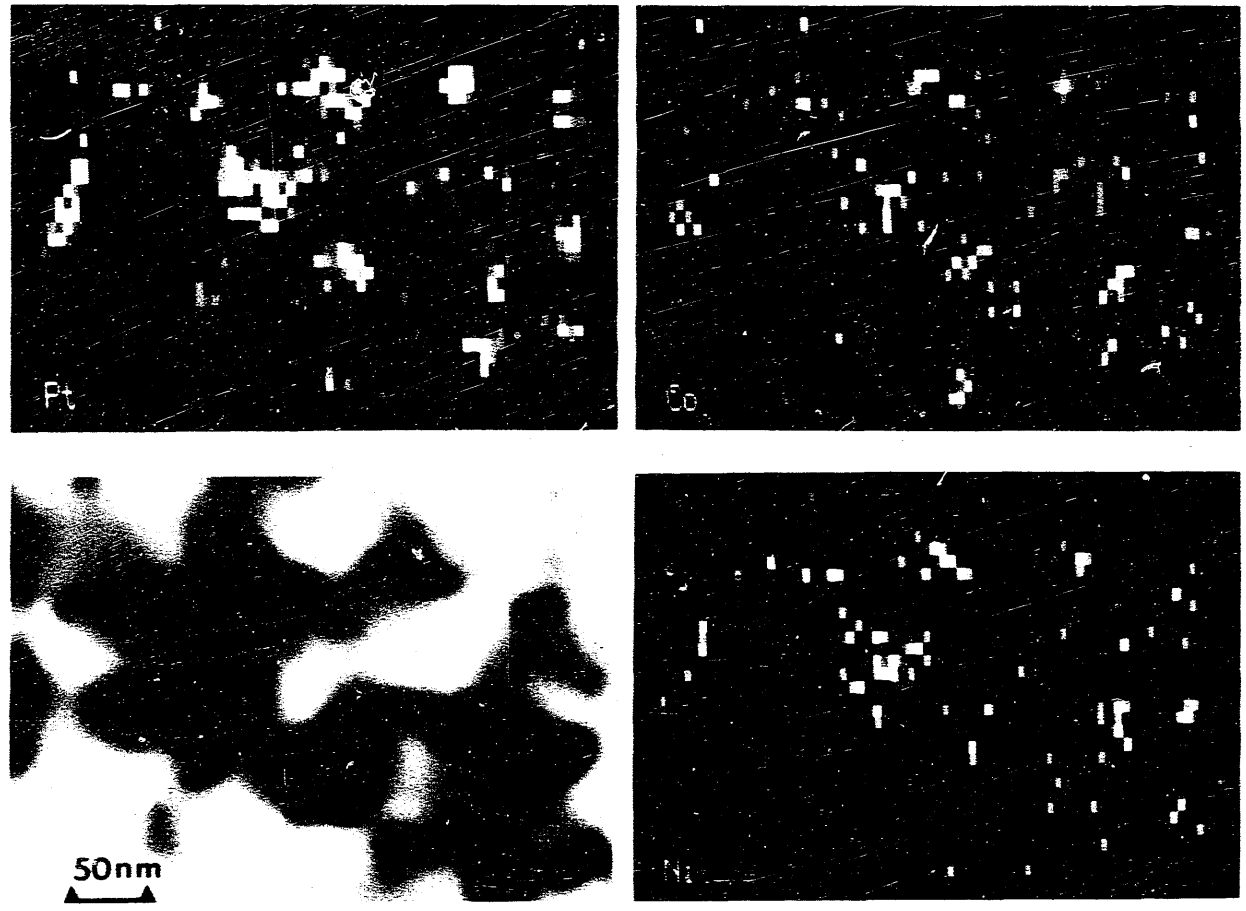


XBB 871-1

Figure 5: (lower left) Secondary electron image of a Pt-Co-Ni catalyst on a carbon black support. Pt:Co:Ni loadings in atomic ratios of 3:1:1. (upper left) and (lower right) X-ray mapping images formed from Pt, Co and Ni characteristic x-ray emission. 30 nm beam at 200 KeV.

# END

# DATE FILMED

4/21/92